Food & Medicine Homology

ISSN 3006-6867 (print); 3006-4252 (online)
https://doi.org/10.26599/FMH.2025.9420073

Research Article

Characteristic components from Rehmannia radix and their effects on insulin resistance through PI-3K/AKT signaling pathway in HepG2 Cells

Zhen-Hua Liu[1,2], Bei-Bei Yu[1,3], Hui-Hui Zhou[1,2], Shi-Shi Zhang[1,3], Xu Yang[1,3], Zhi-Fei Chen[4], Chang-Tong Lu[4], Qiu-Ling Wang[4], Dong-Xu Cheng[4], Yi-Bo Ning[4], Yan-Xia Xiong[5], Guang-Ping Lv[6] (✉), Wen-Yi Kang[1,3] (✉)

[1] *National R & D Center for Edible Fungus Processing Technology, Henan University, Kaifeng 475004, China*
[2] *Functional Food Engineering Technology Research Center, Henan, Kaifeng 475004, China*
[3] *Joint International Research Laboratory of Food & Medicine Resource Function, Kaifeng 475004, China*
[4] *China Tobacco Henan Industrial Company Ltd., Zhengzhou 450000, China*
[5] *Jiangzhong Pharmaceutical Co. Ltd, Nanchang 330004, China*
[6] *School of Food and Pharmaceutical Engineering, Nanjing Normal University, Nanjing 210046, China*

Received: 1 January 2025 / **Revised:** 20 January 2025 / **Accepted:** 22 January 2025

Abstract: *Rehmannia radix* is a kind of food and medicinal material, riched in monoterpenoids, phenylethanol glycosides, triterpenes, flavonoids, and other kinds of chemical compounds, among which monoterpenoids such as iridoids and ionones, and phenylethanol glycosides are the characteristic components of R. radix, with various biological activities. To excavate more characteristic active ingredients, the chemical compositions were identified from the 75% ethanol extract by v a variety of column methods and their hypoglycemic activities were evaluated in HepG2 cells. As a consequence, 13 compounds (**1**-**13**) were identified, including 4 iridoid compounds, 3 ionones, and 6 phenylethanol compounds, among them compound **3** was a new iridoid. The hypoglycemic activity showed that 7 compounds (**1~2**, **4~7** and **13)** could promote glucose uptake of IR-HepG2 cells. And compound **6** could significantly upregulate protein levels of PI-3K, *p*-GSK3*β*, *p*-AKT and GLUT4, and significantly downregulated protein levels of PEPCK and G6Pase. These results revealed that compound **6** improved insulin resistance in HepG2 cells probably by activating PI-3K/AKT signaling pathway and inhibiting gluconeogenesis. These results succeeded in enriching the chemical composition of R. radix and provided an important scientific basis for the application of Rehmannia in the treatment of diabetes.

Keywords: Rehmannia radix; iridoids; ionones; phenylethanol; insulin resistance; HepG2 cells

Citation: Liu Z. H., Yu B. B., Zhou H. H., et al. Characteristic components from Rehmannia radix and their effects on insulin resistance through PI-3K/AKT signaling pathway in HepG2 Cells. *Food & Medicine Homology*, 2025, 2: 9420073. https://doi.org/10.26599/FMH.2025.9420073

1 Introduction

Insulin resistance plays a pivotal role in the development of numerous metabolic disorders, such as type 2 diabetes (T2D)[1]. This resistance can lead to chronically elevated blood glucose levels, which, over time, can cause damage to various organs and systems within the body, such as the kidneys, nerves, and blood vessels. The causes of insulin resistance are multifaceted, encompassing a combination of genetic predispositions and environmental influences, including obesity, physical inactivity, and poor dietary choices. Research has demonstrated that the IRS-1/PI3K/AKT pathway serves is a classical signaling pathway for controlling Insulin resistance in the liver [1,2].

More and more natural products were found to have significant effects on insulin resistance[3]. Anthocyanins from mulberries have been discovered to stimulate the PI3K/AKT signaling pathway, which in turn enhances the phosphorylation of its downstream effector GSK3*β*. This activation subsequently triggers the upregulation of GYS2, a key enzyme in glycogen synthesis, thereby mitigating insulin resistance in HepG2 cells under conditions of high glucose and palmitic acid exposure[4]. Gallic acid increases the expression of PPAR-γ in adipose tissue, liver and skeletal muscle, enhances the activity of tyrosine kinase, promotes IRS phosphorylation, and improves insulin-dependent glucose transport through GLUT4/PI3K/ AKT pathway in adipose tissue, thereby improving IR in rats[5]. Pu *et al.* 's study established that baicalein exerts its inhibitory effect on insulin resistance IR through a dual mechanism: by suppressing the mitogen-activated protein kinase (MAPK) pathway, which is often associated with inflammation and cell proliferation, and by activating the IRS-1/PI3K/AKT signaling pathway, which is central to insulin signaling and glucose metabolism[6].

Address correspondence to Guang-Ping Lv, guangpinglyu@njnu.edu.cn; Wen-Yi Kang, kangweny@hotmail.com

Rehmannia radix (R. radix) is the raw or dehydrated tuber roots of *Rehmannia glutinosa* Libosch from the Scrophulariaceae family. It is predominantly found in Shaanxi, Henan, Shandong, Hebei and other places, and is listed as a versatile resource with applications in both medicinal and culinary domains, and is among the well-known "four Huai medicines"[7]. R. radix is known for its ability to dispel heat and cool the blood, as well as to nourish Yin and generate fluids. It is predominantly employed in the treatment of conditions characterized by pathogenic heat penetrating into the ying and blood aspects of the body, warming toxic hair spots, and internal heat eliminating thirst[7,8]. Over 200 distinct compounds have been extracted and characterized from R. radix, including iridoid, ionones, phenylethanol, lignans, and phenolic acids, etc[9]. Among them, monoterpenes and phenylethanoid glycosides were the characteristic components in R. radix. They exhibited effects on heart-protection[10], immune-regulation[11], hepatoprotective[12], anti-tumor[13] and nephroprotective effects[14]. In order to find more characteristic components with hypoglycemic activities, its chemical compositions and hypoglycemic activity were systematically studied.

As a consequence, a total of 13 distinct compounds had been identified from 75% ethanol extract of R. radix (Fig 1). They were comprising rehmaglutin D **(1)**[15], piscrocin D **(2)**[16], rehmachinin D **(3)**, piscrocin A **(4)**[17], sec-hydroxyaeginetic acid **(5)**[18], trihydroxy-β-ionone **(6)**[19], dihydroxy-β-ionone **(7)**[20], 3,4-dihydroxyphenylethanol **(8)**[21], jionoside C **(9)**[22], leucoseceptoside A **(10)**[23], acteoside **(11)**[24], martynoside **(12)**[25], decaffeoylverbascoside **(13)**[26]. Among them, compound **3** is a new compound. And it was found that compounds **1-2, 4-7** and **13** could enhance glucose uptake in IR-HepG-2 cells to different degrees, and compound **6** had the highest hypoglycemic activity. Western Blot experiments showed that compound **6** could increase the protein levels of GLUT4, *p*-GSK3β , PI3K and *p*-AKT by stimulating the PI3K/AKT signaling pathway. This activation subsequently led to a decrease in the protein levels of G6Pase and PEPCK, which are key enzymes in gluconeogenesis. By promoting glycogen synthesis, compound **6** indirectly suppressed gluconeogenesis and thereby ameliorated insulin resistance.

2 Experimental Section

2.1 Instruments and Reagents

Silica gel grades 200-300 and 300-400 from Qingdao Marine Chemical Inc. (Shandong, China); Sephadex HL-20 with particle sizes of 20-150 μm, and Lichroprep RP18 gel with particle sizes of 40-63 μm, both sourced from Millipore Sigma (Beijing, China) and Amersham Biosciences (Uppsala, Sweden).; Flash chromatography (Biotage, Sweden), HPLC (High Performance Liquid chromatography) and Semi-Prep HPLC (Semi-preparative HPLC) were performed using the Shimadzu LC-20AP system (Japan) and Agilent Technologies, Inc (CA, USA). NMR (Nuclear magnetic resonance) spectroscopic data were obtained on a Bruker AM-400 (Bremerhaven, Germany) at 500 MHz for ^{1}H NMR and 100 MHz for ^{13}C NMR. MS (Mass spectrometry) MDS Sciqaszex (Concord, Ontario, Canada).

HepG2 cells produced by Procell Life Science&Technology Co.,Ltd., Wuhan, China, were used in this experiment. Full wavelength enzyme label (Thermo Fisher, Type 1510); CO_2 incubator (Thermo scientific, 3111); Centrifugal precipitator (Shanghai surgical instrument factory, 800); Multicolor

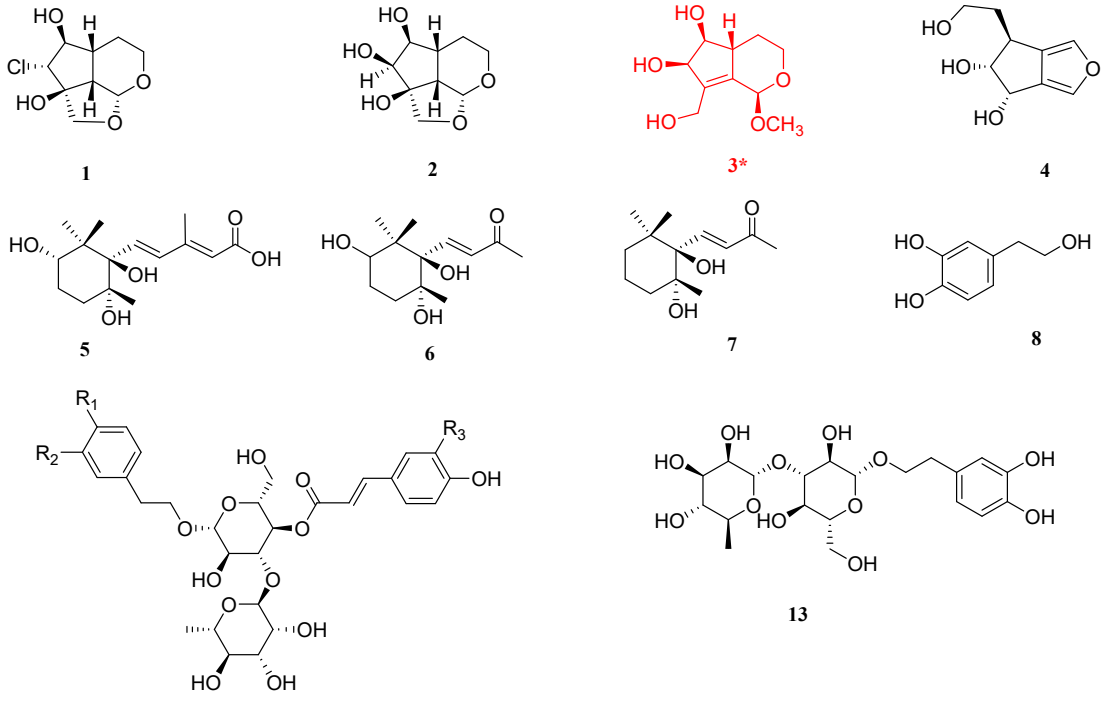

Figure 1 Structures of compounds 1-13 from R. radix.

fluorescence, chemiluminescence and optical imager (ProteinsiMple FluorcheM Q); Mini desktop refrigerated centrifuge TherMo (D-37520); Electrophoresis apparatus (EPS600 Tanon); Trypsin digestion liquid (Shanghai Biyuntian Biotechnology Co., LTD.); Glucose determination kit rongsheng biological pharmaceutical co., LTD. (Shanghai); BCA protein concentration determination kit (Beijing Solaibao Technology Co., LTD.).

2.2 Experimental Materials

The sample R. radix was collected in Henan Province in June 2022 and identified by Prof. Li Changqin of Henan University. The voucher specimen (No.20211012) was stored in the national R & D Center for Edible Fungus Processing Technology, Henan University, Kaifeng 475004, China.

2.3 Extraction and Isolation

Twenty kilogram of dry R. radix, crush, soaked in 75% ethanol (50 L) for 2 times, with the sample being maintained at room temperature for a duration of 7 days during each trial. Combine the extract, concentrate under reduced pressure until there is no alcohol taste, and get a total extract of about 6500 g. After the total extract of R. radix was dissolved with appropriate amount of water, the extraction process involved using petroleum ether, ethyl acetate, and n-butanol, respectively. Following the extraction, the mixtures were concentrated under reduced pressure to obtain petroleum ether layer (Fr.A), ethyl acetate layer (Fr.B) and n-butanol layer (Fr.C).

Using mobile phase DCM and DCM/MeOH (30:1~1:1, *v/v*), Fr.B (79.1 g) was eluted by ordinary silica gel column chromatography yielded **4** components (Fr.B-1~Fr.B-4).

Fr.B-1 (6.8 g) was separated by Flash silica gel column chromatography, eluted by PE/EtOAc (6:1~1:10, *v/v*) , this procedure yielded fractions Fr.B-1-1 and Fr.B-1-2. Subsequently, Fr.B-1-1 was further purified on a normal silica gel column using a mobile phase DCM/MeOH (150:1~1:1, *v/v*) to obtain compound **7** (113 mg).

Fr.B-2 (4.1 g) was separated by normal phase silica gel column chromatography, eluted by mobile phase PE/EtOAc (1:1~1:30, *v/v*), and combined by TLC detection to obtain 4 subcomponents (Fr.2-1~Fr.2-4). Fr.B-2-1 and Fr.B-2-2 were purified by Sephadex LH-20 gel column chromatography (mobile phase: MeOH) to obtain compound **8** (52 mg). Fr.B-2-3 was purified by Sephadex LH-20 gel column chromatography (mobile phase: MeOH) to obtain compound **6** (22 mg).

Fr.B-3 (1.5 g) was separated by normal silica gel column chromatography, and the mobile phase was PE/EtOAc (4:3~1:30, *v/v*). After TLC detection, the same components were combined to obtainFr.B3-1, Fr.B3-2, Fr.B3-3.The compound **5** (107 mg) was obtained by elution of Fr.B-3-1 with Sephadex LH-20 gel column chromatography (mobile phase: MeOH).

Fr.B-4 (3.5 g) was separated by Flash silica gel column chromatography, eluted by mobile phase PE/EtOAc (2:3~1:20, *v/v*), and detected by TLC to obtain Fr.B4-1. Fr.B-4-1 was eluted by Sephadex LH-20 gel column chromatography (mobile phase: MeOH) to obtain Fr.B-4-1-1 and Fr.B-4-1-2. Fr.B-4-1-1 was eluted with mobile phase DCM/MeOH (10:1~1:30, *v/v*) by normal phase silica gel column chromatography to obtain compound **1** (48 mg). The compound **9** (33 mg) was obtained by elution of Fr.B-4-1-2 with mobile phase PE/EtOAc (1:1~1:20, *v/v*) using a silica gel column (under pressure).

Fr.C (272.5 g) was separated by silica gel column chromatography and eluted with mobile phase DCM/MeOH (30:1~1:1, *v/v*). After TLC detection, Fr.C-1to Fr.C-5 were obtained.

Fr.C-1 (2.3 g) was separated by Flash silica gel column chromatography, eluted with mobile phase PE/EtOAc (1:3~1:30, *v/v*), and combined with the same components after TLC detection, then Fr.C-1-1 was obtained. The compound **2** (33 mg) was obtained by elution of Fr.C-1-1 with Sephadex LH-20 gel column chromatography (mobile phase: MeOH).

Fr.C-2 (4.4g) was separated by Flash silica gel column chromatography, eluted with mobile phase PE/EtOAc (1:3~1:30, *v/v*), and combined with the same components after TLC detection to obtain Fr.C-2-1~Fr.C-2-3. Fr.C-2-1 was eluted with mobile phase PE/EtOAc (1:8~1:30, *v/v*) and compounds **11** (460 mg) were obtained by TLC detection. Fr.C-2-2 was further purified by Sephadex LH-20 gel column chromatography (mobile phase: MeOH) to obtain compound **12** (25 mg). Fr.C-2-3 was separated by Sephadex LH-20 gel column chromatography, eluted with mobile phase MeOH, then semi-prepared HPLC was used to further purify by mobile phase MeOH/H_2O (51:49, *v/v*). Compound **10** (6 mg) was obtained.

Fr.C-3 (6.8 g) was separated by Flash silica gel column chromatography, eluted with mobile phase EtOAc/MeOH (10:1~1:30, *v/v*), and combined with the same components after TLC detection to obtain Fr.C-3-1 and Fr.C-3-2. By Fr.C-3-1 was further purified using Sephadex LH-20 gel column chromatography (mobile phase: MeOH), and silica gel column (pressurized) with mobile phase PE/EtOAc (3:1), and compound **4** (37 mg) was obtained.

Fr.C-4 (22.2 g) was separated by Flash silica gel column chromatography, with mobile phase of EtOAc/MeOH (8:1~1:30, *v/v*) gradient elelation to obtain Fr.C-4-1. Fr.C-4-1 was eluted by a normal silica gel column with mobile phase EtOAc/MeOH (7:1, *v/v*) to obtain compound **13** (15 mg). The compound **13** (15 mg) was obtained by elution of Fr.C-1-1 mobile phase EtOAc/MeOH (7:1, *v/v*) using a normal silica gel column.

Fr.C-5 (4.3 g) was separated by Flash silica gel column chromatography, eluted with mobile phase PE/EtOAc (3:2~1:30, *v/v*), and combined with the same components by TLC detection to obtain Fr.C-5-1. Fr.C-5-1 was separated by silica gel column chromatography, eluted with mobile phase DCM/MeOH (30:1~1:1, *v/v*), and then eluted with mobile phase PE/EtOAc (1:1~1:30, *v/v*) through silica gel column (pressurized). Compound **3** (10 mg) was obtained.

2.4 Spectral Data of Compounds

Spectral data for known compounds can be found in support materials.

2.5 Cell Culture

HepG2 cells were cultured in Minimum Essential Medium (MEM) supplemented with 10% fetal bovine serum (FBS) and 1% triple antibiotics, which included penicillin, streptomycin, and amphotericin, to prevent bacterial contamination. The cells were maintained in a humidified atmosphere containing 5% CO_2 at 37 °C to ensure optimal growth conditions. For the subsequent experiment, cells in the logarithmic growth phase were selected and inoculated into 96-well plates at a density of 5 cells per mL. These plates were then incubated in a constant temperature incubator for 24 h to allow for cell attachment and further growth.

2.6 Cell Viability Assay

HepG2 cells of logarithmic growth stage were inoculated into 96-well plates with a density of 5 cells /mL and incubated in a constant temperature incubator for 24 h. After 24 h, the blank group was replaced with a new complete medium, and the cells were treated with compounds **1**-**2**, **4**-**7**, and **13** (200, 100, 50, 25, and 12.5 μmol/L), respectively, while the control group was given equal amounts of serum-free DMEM without compounds. After incubating in the incubator for 48 h, 10 μL of MTT solution with a concentration of 5 mg/mL was added to each well. After 4 h, the supernatant was carefully sucked out, and 100 μL of DMSO was added to each well, incubated in the oven at 37 ℃ for 10 minutes, and then the OD value was determined at the wavelength of 490 nm after being shaken and mixed with an enzyme label. The results were analyzed after the experiment was repeated for 3 times.

2.7 Glucose Uptake Assay

HepG2 cells were cultured in complete MEM medium supplemented with 10% fetal bovine serum and 1% penicillin-streptomycin. When cell fusion reached around 80%, they were carefully and evenly seeded at a density of 4×10^5 cells/mL in a 96 well plate and placed in a 37 ℃, 5% CO_2 incubator for cultivation. After approximately 24 h, the cells adhered to the surface, and the MEM was completely removed, the new DMEM medium was added, and the cells were starved for 12 h. After 12 h, the original growth medium for the blank control group was replaced with fresh MEM complete medium, and the model group was replaced with MEM complete medium containing 8 mmol/L GlcN[27]. After 24 h of modeling induced by the above method, the supernatant was removed, the blank control group and the GlcN modeling group were replaced with the new DMEM medium, and the positive drug group was replaced with the DMEM medium embracing 50 μM rosiglitazone (ROSI). The compound treatment group was replaced with DMEM media containing compounds **1, 2, 4**-**7** and **13** (200, 100, 50, 25 and 12.5 μmol/L), which were cultured in the incubator for 48 h, and the glucose content in the cell supernatant was measured using the GOD-POD method, and the glucose uptake by the cells during this period was calculated. Statistical analysis was performed to assess the significance of the differences between the blank group and the model group, allowing for the determination of the optimal concentration and duration for modeling.

2.8 Western Blot

The total protein was extracted from the cells, the protein concentration was measured according to the instructions provided in the BCA protein concentration determination kit, and the absorbance value of 562 nm wavelength was detected by enzyme-labeled instrument (Full wavelength enzyme labeling instrument, Thermo Fisher). The standard curve was generated following the instructions, and the protein concentration was calculated accordingly. Western Blot was performed according to the experiment accomplished by Liu *et al*[28].

2.9 Statistical Analysis

One-way ANOVA was performed using SPSS 19.0 software to analyze the experimental results, which are presented as the mean with standard deviation. This statistical method allows for the comparison of means across multiple groups to identify any significant differences. Following this analysis, all bar graphs were generated and assessed using GraphPad Prism 7.0 software. In this context, a p-value of less than 0.05 was considered indicative of statistical significance, suggesting that any observed differences among the groups were unlikely to have occurred by chance. This rigorous statistical approach ensures the reliability and validity of the findings obtained from the experiments.

3 Results

3.1 Analysis of New Iridoids

The HR-ESI-MS gives excimer ion peak *m/z*: 239.0891 $[M+Na]^+$ (theoretical value, 239.0890), combined with NMR spectra, therefore the molecular formula is derived as $C_{10}H_{16}O_5$. The absorption at 3410 cm^{-1} in IR spectrum indicates the presence of hydroxyl groups in the molecule. The ^{1}H-NMR spectra contain one methoxy-matrix signal [δ_H 3.33 (3H, s, H-11)] and one acetal signal [δ_H 5.30 (1H, s, H-1)]. The ^{13}C-NMR spectrum contains 10 carbon atoms, including one methoxy signal [(δ_C 54.76, C-11)], and the remaining 9 carbon signals include one oxygenated methylene (δ_C 56.7, C-10), three oxygenated methylenes [δ_C 79.6, (C-6)), δ_C 74.5, (C-7) , and δ_C 96.3 (C-1)], one pair of terminal double bond signals [δ_C 137.6, (C-9)] and [δ_C 138.3, (C-8)].

The above data indicate that the compound is a typical iridoid compound, with C-8 and C-9 being two olefin carbons, and C-6, C-7, and C-10 having hydroxyl substituents. The ^{1}H-NMR and ^{13}C-NMR data of compound **3** were similar to that of rehmachinin A [29] except that compound **3** has one methoxy group [δ_H 3.33 (3H, s, H-11), δ_C 54.8 (C-11)] (**Table 1**). The correlation between [δ_H 3.33 (3H, s, H-11)] and [δ_C 100.31 (C-1)] was found in HMBC, and it was determined that the methoxy group was linked to C-1. The correlations of [δ_H 3.58 (1H, m) and H-3] and [(δ_C 32.92, C-4), (δ_C, 96.30 C-1), (δ_C 46.00, C-5)]; [δ_H 4.24 (1H, d, J = 13.3 Hz, H-10 a), 4.09 (1H, dd, J = 2.7, 13.3 Hz), H-10b] and [δ_C 138.26, (C-8)] confirmed the above speculation (**Fig 2**). In summary, the structural identification of compound **3** is as follows: (1*R*,4a*R*,6*S*,7*R*)-1,3,4,4a,6,7-hexahydro-8-(hydroxymethyl) cyclopenta[c] Pyran-1-methoxyl-6,7-diol, named rehmachinin D.

Table 1 The ^{1}H and ^{13}C-NMR data of compound 3 (CD_3OD, δ in ppm, J in 500MHz)

Position	δ_H	δ_C
1	5.30(1H, s)	96.3
3	3.58 (1H, m) 3.79 (1H, t, J = 11.2 Hz)	59.4
4	1.38(1H, ddd, J = 4.6,12.6,25.0 Hz) 2.07(1H, dd, J = 6.0,1.3 Hz)	32.9
5	2.72 (1H, s)	46.0
6	3.63 (1H, t, J = 5.9 Hz)	79.6
7	4.35（1H, d, J = 6.0 Hz）	74.5
8		138.3
9		137.6
10	4.24 (1H, d, J = 13.3 Hz) 4.09 (1H, dd, J = 2.7,13.3 Hz)	56.7
11	3.33(3H, s)	54.8

3.2 Spectral data of isolated compounds

Rehmantin (**1**), pale yellow powder, *m/z*: 220.05, molecular formula: $C_9H_{13}ClO_4$. ^{1}H-NMR (CD_3OD, 400 MHz) δ_H: 5.31 (1H, d, J = 5.4 Hz, H-1), 4.40 (1H, d, J = 10.3 Hz, H-10a), 4.07 (1H, dd, J = 1.3, 10.0 Hz, H-7), 3.87 (1H, dt, J = 6.3, 3.2 Hz, H-6), 3.82 (1H,

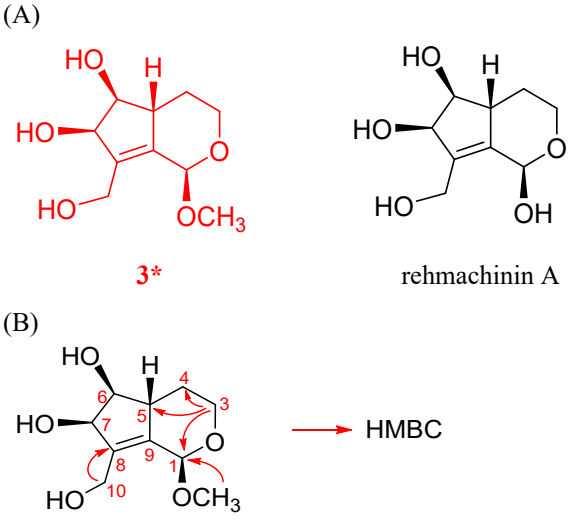

Figure 2 (A) Structure of compounds 3 and rehmachinin A, (B) Key HMBC correlations of compound 3.

dd, *J* = 9.3, 6.6 Hz, H-3a), 3.54 (1H, ddd, *J* = 11.6, 5.1, 1.8 Hz, H-3b), 3.42 (1H, dd, *J* = 10.3, 1.4 Hz, H-10b), 2.30 (1H, dd, *J* = 10.2, 5.4 Hz, H-9), 2.15 (1H, td, *J* = 10.2, 5.7 Hz, H-5), 1.78 (1H, m, H-4b), 1.66 (1H, dd, *J* = 14.2, 1.6 Hz, H-4a)。 ^{13}C-NMR (CD_3OD, 101 MHz) δ_C: 101.4 (C-1), 85.2 (C-8), 76.2 (C-6), 74.1 (C-7), 72.7 (C-10), 56.5 (C-3), 45.9 (C-9), 36.7 (C-5), 22.0 (C-4).

Piscrocin D (**2**), Brownish-yellow oily, *m/z*: 202.08, molecular formula: $C_9H_{14}O_5$. ^{1}H-NMR (CD_3OD, 400 MHz) δ_H: 5.30 (1H, d, *J* = 5.5 Hz, H-1), 3.95 (1H, dd, *J* = 3.5, 11.2 Hz, H-6), 3.89 (1H, dd, *J* = 2.2, 12.2 Hz, H-3a), 3.78 (1H, d, *J* = 10.1 Hz, H-10b), 3.70 (1H, d, *J* = 3.7 Hz, H-7), 3.62 (1H, d, *J* = 10.1 Hz, H-10a), 3.51 (1H, ddd, *J* = 1.2, 5.1, 11.8 Hz, H-3b), 2.45 (1H, m, H-5), 2.18 (1H, dd, *J* = 5.5, 10.3 Hz, H-9), 1.78 (1H, m, H-4b), 1.62 (1H, brdd, *J* = 1.8, 12.0 Hz, H-4a)。 ^{13}C-NMR (CD_3OD, 101 MHz) δ_C: 102.0 (C-1), 85.5 (C-8), 79.3 (C-7), 75.4 (C-10), 74.0 (C-6), 56.2 (C-3), 46.6 (C-9), 37.2 (C-5), 22.1 (C-4)。

Compound **3**, rehmachinin D, light yellow oily, m/z: 216.09, ESI-MS m/z 239 $[M+Na]^+$. HR-ESI-MS (m/z) 239.0891 $[M+Na]^+$ ($C_{10}H_{16}O_5Na$, 239.0895). V(MeOH) λ_{max} (logε) 206 (0.407) nm. IR (KBr) ν_{max} 3410 cm^{-1}. ^{1}H and ^{13}C NMR data, see Table 1.

Piscrocin A (**4**), Oily brown, *m/z*: 184.07, molecular formula: $C_9H_{12}O_4$. ^{1}H-NMR (CD_3OD, 400 MHz) δ_H: 7.41 (1H, s, H-1), 7.23 (1H, s, H-3), 4.77 (1H, d, *J* = 4.9 Hz, H-7), 3.92 (1H, dt, *J* = 3.6, 7.2 Hz, H-6), 3.79 (2H, m, H-10), 2.93 (1H, m, H-5), 2.02 (1H, td, *J* = 3.6, 7.3 Hz, H-9b), 1.77 (1H, m, H-9a)。 ^{13}C-NMR (CD_3OD, 101 MHz) δ_C: 137.4 (C-1), 135.6 (C-3), 132.2 (C-4), 131.0 (C-8), 85.5 (C-6), 68.1 (C-7), 62.1 (C-10), 40.9 (C-5), 36.5 (C-9).

Sec-hydroxyaeginetic acid (**5**), Light yellow crystalline, *m/z*: 284.16, molecular formula: $C_{15}H_{24}O_5$. ^{1}H-NMR (CD_3OD, 400 MHz) δ_H: 6.70 (1H, d, *J* = 16.0 Hz, H-7), 6.39 (1H, d, *J* = 16.0 Hz, H-8), 5.81 (1H, s, H-10), 3.74 (1H, brs, H-2), 2.32 (3H, d, *J* = 1.0 Hz, CH_3-9), 1.93 (1H, m, H-3*α*), 1.93 (1H, m, H-4*β*), 1.53 (1H, m, H-3*β*), 1.53 (1H, m, H-4*α*), 1.12(3H, s, 1*α*-CH_3), 1.04(3H, s, 5-CH_3), 0.89 (3H, s,1*β*-CH_3)。 ^{13}C-NMR (CD_3OD, 101 MHz) δ_C: 170.8 (C-11), 153.8 (C-9), 139.5 (C-7), 134.6 (C-8), 119.7 (C-10), 82.2 (C-6), 75.6 (C-5), 74.5 (C-2), 44.8 (C-1), 36.0 (C-4), 27.7 (C-3), 27.0 (5-CH_3), 23.0 (1*α*-CH3), 18.0 (1*β*-CH3), 14.2 (9-CH_3).

Trihydroxy-*β*-ionone (**6**), White powder, *m/z*: 242.15, molecular formula: $C_{13}H_{22}O_4$. ^{1}H-NMR (CD_3OD, 400 MHz) δ_H: 7.43 (1H, d, *J* = 16.3 Hz, H-7), 6.30 (1H, d, *J* = 16.3 Hz, H-8), 3.74 (1H, brs, H-2), 2.32 (3H, s, H-10),1.94 (1H, m, H-3*α*), 1.94 (1H, m, H-4*β*), 1.54 (1H, m, H-3*β*), 1.54 (1H, m, H-4*α*), 1.15(3H, s, 1*α*-CH_3), 1.05(3H, s, 5-CH_3), 0.89 (3H, s, 1*β*-CH_3)。 ^{13}C-NMR (CD_3OD, 101 MHz) δ_C: 201.5 (C-9), 152.8 (C-7), 132.0 (C-8), 82.4 (C-6), 75.4 (C-5), 74.3 (C-2), 44.9 (C-1), 36.0 (C-4), 27.6 (C-3), 27.0 (C-10), 27.0 (5-CH_3), 23.0 (1*α*-CH_3), 18.3 (1*β*-CH_3).

Dihydroxy-*β*-ionone (**7**), Pale yellow powder, *m/z*: 226.15, molecular formula: $C_{13}H_{22}O_3$. ^{1}H-NMR (CD_3OD, 400 MHz) δ_H: 7.43 (1H, d, *J* = 16. 2 Hz, H-7), 6.33(1H, d, *J* = 16.2 Hz, H-8), 2.32 (3H, s, H-10), 1.89 (1H, m, H-3a), 1.80 (1H, m, H-4b), 1.70 (1H, m, H-2b), 1.48 (1H, m, H-4a), 1.40 (1H, m, H-3b), 1.25 (3H, s, 1*α*-CH_3), 1.18 (1H, m, H-2a), 1.07 (3H, s, 5-CH_3), 0.81 (3H, s, 1*β*-CH_3)。 ^{13}C-NMR (CD_3OD, 101 MHz) δ_C: 201.4 (C-9), 153.3 (C-7), 131.8 (C-8), 80.6 (C-6), 75.5 (C-5), 39.6 (C-1), 37.3 (C-2), 36.6 (C-4), 27.4 (1*β*-CH_3), 27.4 (C-10), 27.0 (5-CH_3), 25.8 (1*α*-CH_3), 18.91 (C-3).

3,4-Di-hydroxyphenylethanol (**8**), Oily brown, *m/z*: 154.06, molecular formula: $C_8H_{10}O_3$. ^{1}H-NMR (CD_3OD, 400 MHz) δ_H: 6.67 (1H, d, *J* = 8.0 Hz H-5), 6.65 (1H, d, *J* = 1.9 Hz, H-2), 6.52 (1H, dd, *J* = 8.0, 2.0 Hz, H-6), 3.67 (2H, t, *J* = 7.2Hz, H-8), 2.66 (2H, t, *J* = 7.2Hz, H-7)。 ^{13}C-NMR (CD_3OD, 101 MHz) δ_C: 146.1 (C-3), 144.6 (C-4), 131.7 (C-1), 121.2 (C-6), 117.0 (C-5), 116.3 (C-2), 64.5 (C-8), 39.6 (C-7).

Jionoside C (**9**), Light yellow oily, *m/z*: 592.21, molecular formula: $C_{29}H_{36}O_{13}$. ^{1}H-NMR (CD_3OD, 400 MHz) δ_H: 7.59 (1H, d, *J* = 15.8 Hz, H-7′), 7.27 (4H, d, *J* = 4.3 Hz, H-2, 3, 5, 6), 7.18 (1H, m, H-4), 7.06 (1H, d, *J* = 1.9 Hz, H-2′), 6.96 (1H, dd, *J* = 1.9, 8.2 Hz, H-5′), 6.78 (1H, d, *J* = 8.1 Hz, H-6′), 6.28 (1H, d, *J* = 15.8 Hz, H-8′), 5.19 (1H, d, *J* = 1.4 Hz, rha-H-1), 4.39 (1H, d, *J* = 7.8 Hz, glc-H-1), 2.95 (2H, t, *J* = 7.2 Hz, H-7), 1.09 (3H, d, *J* = 6.1 Hz, rha-H-6)。 ^{13}C-NMR (CD_3OD, 101 MHz) δ_C: 168.3 (C-9′), 149.7 (C-4′), 148.0 (C-8′), 146.6 (C-3′), 140.0 (C-1), 130.1 (C-3), 130.1 (C-5), 129.4 (C-2), 129.4 (C-6), 127.6 (C-1′), 127.2 (C-4), 123.3 (C-6′), 116.6 (C-5′), 115.2 (C-7′), 114.6 (C-2′), 104.3 (glc-C-1), 103.1 (rha-C-1), 81.7 (glc-C-3), 76.2 (glc-C-2), 76.1 (glc-C-5), 73.8 (rha-C-4), 72.3 (C-1), 72.0 (rha-C-2), 71.9 (rha-C-3), 70.6 (rha-C-5), 70.4 (glc-C-4), 62.4 (glc-C-6), 37.2 (C-1), 18.5 (rha-C-6).

Leucoseceptoside A (**10**), Yellowish brown oily, *m/z*: 638.22, molecular formula: $C_{30}H_{38}O_{15}$. ^{1}H-NMR (CD_3OD, 400 MHz) δ_H: 7.66 (1H, d, *J* = 15.9 Hz, H-7′), 7.20 (1H, d, *J* = 1.0 Hz, H-2′), 7.09 (1H, d, *J* = 8.1, 1.0 Hz, H-6′), 6.82 (1H, d, *J* = 8.1 Hz, H-5′), 6.70 (1H, d, *J* = 1.0 Hz, H-2), 6.68 (1H, d, *J* = 8.4 Hz, H-5), 6.56 (1H, d, *J* = 8.0, 1.0 Hz, H-6), 6.33 (1H, d, *J* = 15.8 Hz, H-8′), 5.20 (1H, s, rha-H-1), 4.90 (1H, t, *J* = 9.2 Hz, glc-H-4), 4.38 (1H, d, *J* = 8.1 Hz, glc-H-1), 3.89 (3H, s, 3′-OCH_3), 1.13 (3H, dd, *J* = 6.2, 23.7 Hz, rha-H-6)。 ^{13}C-NMR (CD_3OD, 101 MHz) δ_C: 168.2 (C-9′), 150.6 (C-3′), 149.4 (C-4′), 148.0 (C-7′), 146.0 (C-4), 144.7 (C-3), 131.4 (C-1), 127.7 (C-1′), 124.3 (C-6′), 121.2 (C-6), 117.2 (C-5), 116.5 (C-5′), 116.2 (C-2), 115.0 (C-8′), 111.9 (C-2′), 104.2 (glu-C-1′), 103.1 (rha-C-1), 81.5 (glu-C-3), 76.2 (glu-C-5), 76.0 (glu-C-2), 73.7 (rha-C-4), 72.3 (rha-C-3), 72.3 (rha-C-2), 72.0 (C-8), 70.6 (rha-C-5), 70.4 (glu-C-4), 62.4 (glu-C-6), 56.5 (3′ -OCH_3), 36.6 (C-7), 18.5 (rha-C-6).

Acteoside (**11**), Reddish brown oily, *m/z*: 634.20, molecular formula: $C_{29}H_{36}O_{15}$. ^{1}H-NMR (CD_3OD, 400 MHz) δ_H: 7.60 (1H, d, *J* = 15.8 Hz, H-7′), 7.06 (1H, d, *J* = 1.9 Hz, H-2′), 6.96 (1H, dd, *J* = 8.3, 1.9 Hz, H-6′), 6.78 (1H, d, *J* = 8.2 Hz, H-5′), 6.70 (1H, d, *J* = 2.0 Hz, H-2), 6.68 (1H, d, *J* = 8.0 Hz, H-5), 6.57 (1H, dd, *J* = 8.0, 2.0 Hz, H-6), 6.28 (1H, d, *J* = 15.9 Hz, H-8′), 5.19 (1H, d, *J* = 1.4 Hz, rha-H-1), 4.89 (1H, t, *J* = 9.1 Hz, glc-H-4), 4.38 (1H, d, *J* = 8.0 Hz, glc-H-1), 1.10 (3H, d, *J* = 6.18 Hz, rha-H-6)。 ^{13}C-NMR (CD_3OD, 101 MHz) δ_C: 168.2 (C-9′), 146.8 (C-3′), 149.7 (C-4′), 148.0 (C-7′), 144.6 (C-4), 146.0 (C-3), 131.4 (C-1), 127.6 (C-1′), 123.2 (C-6′), 121.2 (C-6), 116.3 (C-5), 116.5 (C-5′), 117.1 (C-2),

114.6 (C-8′), 115.2 (C-2′), 104.2 (glu-C-1), 103.0 (rha-C-1), 81.7 (glu-C-3), 76.1 (glu-C-5), 75.9 (glu-C-2), 73.7 (rha-C-4), 72.0 (rha-C-3), 72.2 (rha-C-2), 72.3 (C-8), 70.5 (rha-C-5), 70.4 (glu-C-4), 62.3 (glu-C-6), 36.5 (C-7), 18.4 (rha-C-6).

Martynoside (**12**), Pale yellow fat, *m/z*: 652.23, molecular formula: $C_{31}H_{42}O_{15}$. ^{1}H-NMR (CD_3OD, 400 MHz) δ_H: 7.65 (1H, d, *J* = 15.8 Hz, H-7′), 7.18 (1H, d, *J* = 1.5 Hz, H-2′), 7.07 (1H, dd, *J* = 1.58, 8.24 Hz, H-6′), 6.80 (1H, d, *J* = 8.4 Hz, H-5′), 6.80 (1H, d, *J* = 8.4 Hz, H-5), 6.73 (1H, d, *J* = 1.9 Hz, H-2), 6.67 (1H, dd, *J* = 1.9, 8.1 Hz, H-6), 6.37 (1H, d, *J* = 15.9 Hz, H-8′), 5.20 (1H, d, *J* = 1.1 Hz, rha-H-1), 4.92 (1H, t, *J* = 9.0 Hz, glc-H-4), 4.37 (1H, d, *J* = 7.9 Hz, glc-H-1), 3.87 and 3.79(3H, s, 2×Ar-OCH3), 2.81 (2H, t, *J* = 6.6 Hz, H-7)1.10 (3H, d, *J* = 6.20 Hz, rha-H-6)。 ^{13}C-NMR (CD_3OD, 101 MHz) δ_C: 168.2 (C-9′), 150.7 (C-4′), 149.3 (C-3′), 147.9 (C-7′), 147.5 (C-3), 147.3 (C-4), 132.9 (C-1), 127.6 (C-1′), 124.3 (C-6′), 121.2 (C-6), 117.0 (C-5), 116.5 (C-5′), 115.1 (C-8′), 112.8 (C-2), 111.7 (C-2′), 104.1 (glu-C-1), 103.0 (rha-C-1), 81.5 (glu-C-3), 76.1 (glu-C-2), 76.0 (glu-C-5), 73.7 (rha-C-3), 72.3 (rha-C-2), 72.1 (C-8), 72.0 (rha-C-3), 70.6 (glu-C-4), 70.4 (rha-C-5), 62.3 (glu-C-6), 56.4 (3′ -OCH_3), 56.4 (4-OCH_3), 36.5 (C-7), 18.4 (rha-C-6).

Decaffeoylverbascoside (**13**), Oily yellow, *m/z*: 464.15, molecular formula: $C_{19}H_{28}O_{13}$. ^{1}H-NMR (CD_3OD, 400 MHz) δ_H: 6.65 (1H, d, *J* = 1.7 Hz, H-2), 6.63 (1H, d, *J* = 8.0 Hz, H-5), 6.50 (1H, dd, *J* = 8.0, 1.7 Hz, H-6), 5.12 (1H, s, rha-H-1), 4.26 (1H, d, *J* = 7.9 Hz, glc-H-1), 3.98 (1H, d, *J* = 7.5 Hz, rha-H-2), 3.95 (1H, dd, *J* = 4.7, 8.0 Hz, rha-H-5), 3.91 (1H, d, *J* = 2.8 Hz, glc-H-6), 3.83 (1H, dd, *J* = 1.7, 11.8 Hz, glc-H-4), 3.66 (1H, m, H-8a), 3.63 (1H, m, H-8b), 3.63(1H, t, *J* = 5.8 Hz, glc-H-6b), 3.55 (1H, dd, *J* = 4.8, 11.0 Hz, glc-H-3), 3.47 (1H, m, rha-H-3), 3.37 (1H, d, *J* = 9.5 Hz, glc-H-2), 3.33(1H, m, rha-H-4), 3.24 (1H, m, glc-H-5), 2.74 (2H, m, H-7), 1.24 (3H, d, *J* = 6.2 Hz, rha-H-6)。 ^{13}C-NMR (CD_3OD, 101 MHz) δ_C: 146.1 (C-4), 144.6 (C-3), 131.5 (C-1), 121.2 (C-6), 117.1 (C-2), 116.3 (C-5), 104.2 (glu-C-1), 102.7 (rha-C-1), 84.5 (glu-C-3), 77.8 (glu-C-5), 75.6 (glu-C-2), 74.0 (rha-C-4), 72.3 (rha-C-2), 72.2 (C-8), 72.1 (rha-C-3), 70.2 (rha-C-5), 70.0 (glu-C-4), 62.6 (glu-C-6), 36.5 (C-7), 17.9 (rha-C-6).

3.3 Effects of Compounds on Viability of HepG2 Cell

To determine the non-toxic concentration of the compound, the effects of different concentrations of compounds 1-2, 4-7, and 13 on the viability of HepG2 cells were evaluated by MTT assay. As shown in Fig 3, compared with the control group, compounds 1-2, 4-7, and 13 showed no cytotoxicity in the range of 12.5 μmol/L to 200 μmol/L, but compound 13 showed significant cytotoxicity at 200 μmol/L ($P > 0.05$). Then, 12.5, 25, 50, 100, 200 μmol/L were used in subsequent experiments.

3.4 Effects of Compounds on Glucose Uptake in IR-HepG2 Cells

In Fig 4, compared with the control group, the glucose uptake of the GlcN group was significantly reduced ($P < 0.001$), indicating the successful establishment of the IR-HepG2 model. Compared with the GlcN group, compounds **2** and **7** (12.5 to 200 μmol/L) significantly increased glucose uptake of IR-HepG2 cells. Compounds **1, 5,** and **6** (25-200 μmol/L) also dramatically increase glucose uptake of IR-HepG2 cells, but they showed no significant hypoglycemic activity at 12.5 μmol/L. Furthermore, compounds **4** (50-200 μmol/L) and **13** (100-200 μmol/L) significantly promote glucose uptake of IR-HepG2 cells. These results indicated that selected compounds increase glucose consumption and improve the IR of HepG2 cells. And Compound **6** showed the best activity (EC_{50} = 150 μmol/L).

3.5 Effects of Compound 6 on Proteins Associated with PI-3K/AKT Signaling Pathway

The mechanism of compound **6** was expected to be further explored because of the best activity. Therefore, the mechanism of promoting sugar absorption was further studied by Western blot (**Fig 5**). After treating cells with GlcN, the expression levels of PI-3K and phosphorylated AKT protein decreased, and the expression levels of PEPCK and G6Pase protein increased, indicating that the PI-3K/AKT signaling pathway was blocked and the downstream gluconeogenic signaling pathway of PI-3K/AKT was activated, thereby inhibiting the glycogen synthesis signaling pathway and leading to IR. In Figure 3, compound **6** did not affect the protein levels of AKT and GSK3*β*, but could increase the expression levels of PI-3K, *p*-AKT, GLUT4, and *p*-GSK3*β* protein in IR-HepG2 cells, while reducing the expression levels of PEPCK

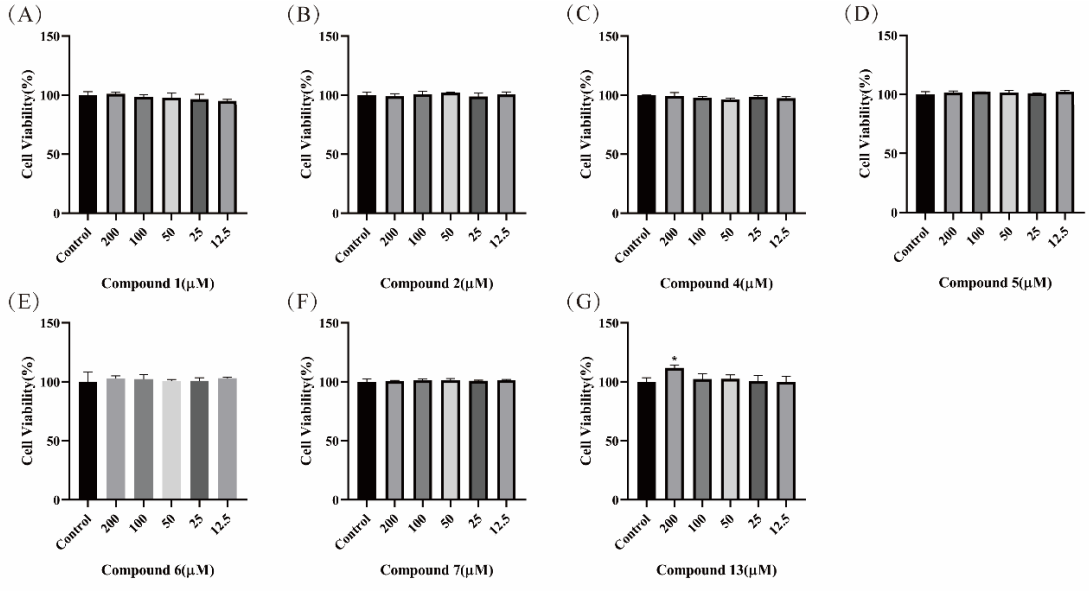

Figure 3 Effects of compounds 1-2, 4-7, and 13 on the HepG2 cell viability. Data presented are the mean ± SD, $n = 3$. Compared with the control group, $^*P < 0.05$,.

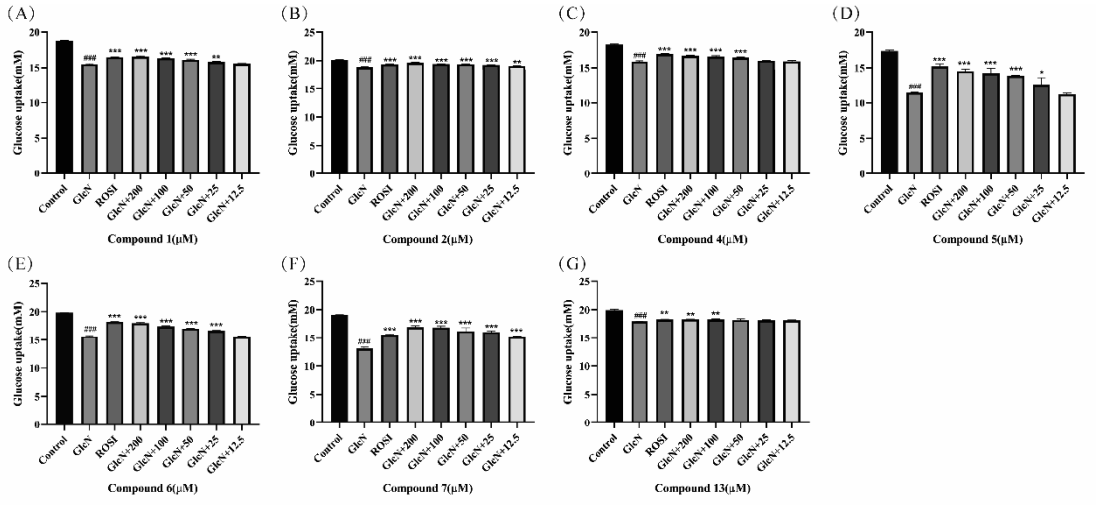

Figure 4 Effects of compounds 1-2, 4-7 and 13 on glucose uptake in IR-HepG2 cells. Compared with the control group, $^{###}P < 0.001$. Compared with the GlcN group, $^{*}P < 0.05$, $^{**}P < 0.01$, $^{***}P < 0.001$.

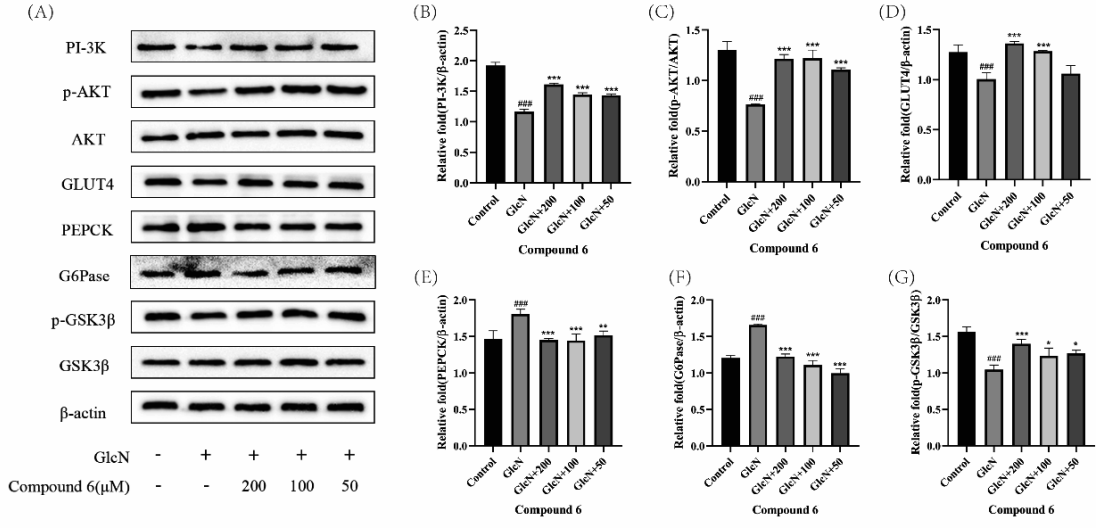

Figure 5 Effects of compound 6 on PI-3K, *p*-AKT, GLUT4, PEPCK, G6Pase and *p*-GSK3β protein expression of IR-HepG2 cells (A-G). Compared with the control group, $^{###}P < 0.001$. Compared with the GlcN group, $^{*}P < 0.05$, $^{**}P < 0.01$, $^{***}P < 0.001$.

protein and G6Pase protein. The results indicated that compound 6 can activate the PI-3K/AKT signaling pathway, stimulate glycogen synthesis, inhibit gluconeogenesis, and thus improve insulin resistance.

Discussion

More than 200 compounds have been isolated from R. radix, including monoterpenoids, phenylethanol glycosides, triterpenoids, flavonoids, lignans, phenolic acids and so on. Among them, monoterpenes and phenylethanol glycosides are the characteristic components of R. radix. The skeletons of monoterpene in R. radix were manily iridoid and ionones, belonging special monoterpenes. The structure of iridoid is unsuitable, which could be degraded during the processing. The change of these compositions is the key factor causing the significant difference of "sex-effect" between the fresh and prepared *Rehmannia glutinosa*. In this experiment, a cumulative total of 13 compounds were isolated and identified from R. radix, including 4 iridoids, 3 ionones and 6 phenylethanol compounds, and compound **3** was a new iridoid.

It was reported that the iridoids derived from R. radix have demonstrated the ability to suppress gluconeogenesis and increase *in vivo* and *in vitro* glycogen synthesis, and these compounds have been shown to mitigate hepatic insulin resistance in mice with type 2 diabetes by activating on PI3K/NOX4/AKT/AMPK signaling pathway[34]. Xu et al. found that catalpol, an iridoid glucoside, has the capacity to decrease blood sugar glucose levels and enhance insulin sensitivity in diabetic mice through the activation of the PI3K/AKT pathway[35]. In addition, myogenesis is enhanced by increasing the expression of myosin heavy chain (MHC), myogenin (MyoG), and myogenic differentiation (MyoD), contributing to activating the AKT/PI3K pathway. Subsequently, Xu's study discovered[36] *et al.* that catalpol is capable of enhancing insulin sensitivity through the activation of the IRS-1/GLUT4 signaling pathway, thereby improving glucose homeostasis in skeletal muscle. Yap's study discovered25[37] *et al* demonstrated that catalpol enhanced the activity of citrate synthase, oxygen consumption and state-3 respiration and increased the protein levels of *p*-AMPK, AKT, IRS-1, GLUT4, AMPK, PI3K, PGC-1*α*, and PPAR-γ. It was speculated that catalpol may activate AMPK/SIRT1/PGC-1*α*/PPAR-*γ* signaling

and the insulin signaling pathway, further improve insulin sensitivity and mitochondrial respiration. Paterinoside and paterinoside A, two iridoids, can inhibit the MAPK and NF-κB pathways, activate the AKT/PI-3K pathway, further improving oxidative stress, and playing a vital role in improving IR[38,39]. An iridoid (4*β*,8*β*)-8-methoxy-3-methyl-10-methylene-2,9-dioxatricyclo[4.3.1.0^{3,7}]decan-4-ol promoted dexamethasone-treated 3T3L-1 lipid metabolism through the activation of the PI3K/AKT signaling pathway. Protein levels of GLUT4, mRNA expression and glucose absorption were upregulated in fatty cells[40].

Therefore, the PI3K/AKT signaling pathway has been clearly identified as the primary pathway through which insulin plays a critical role in liver, adipose tissue, and skeletal muscle[41]. In summary, PI3K/AKT signaling pathway, as a key signaling channel for peripheral insulin action and an important proximal regulator of cell function, plays a pivotal role in regulating the course and progression of T2DM and has great potential. It is one of the important targets that should not be ignored when developing effective therapeutic drugs for T2DM.

In view of this, the hypoglycemic activity of the isolated compounds and their mechanisms were evaluated. Literatures review found that compound **9** has antitumor and *α*-glucosidase inhibitory effect[31,33], compound **10** has anti-inflammatory and *α*-glucosidase inhibitory effects[30,31], compound **11** was found to have a variety of biological activities, including anti-inflammatory, anti-tumor and anti-oxidation, and has inhibitory effects on LPS-induced human umbilical vein endothelial cells and TH22 cells, and compound **12** has antitumor effects[32]. In our study, it was found compounds **1**, **2**, **5**-**7**, **13**-**14** had different degrees of hypoglycemic activity. And compound **6** was found to have hypoglycemic activity by activating the PI3K-AKT pathway. Furthermore, there are few studies on the activity of compounds **3**, **6** and **7**, and their pharmacological effects need to be further developed and utilized.

In this study, we only took HepG2 cells as the research object to preliminarily explore the hypoglycemic effect of compound **6**. However, as an *in vitro* model, the physiological environment and metabolic process of HepG2 cells are quite different from the actual conditions *in vivo*. Therefore, the conclusions drawn from this cell experiment are relatively limited, and it is difficult to fully and accurately reflect the hypoglycemic mechanism, efficacy intensity and potential toxic and side effects of compound **6** in real organisms. In order to make up for this deficiency and make the research results more scientific and convincing, it is urgently needed to carry out further in vivo experiments on compound **6**. By conducting experiments in animal models, whose physiological environment is more closer to the human body, and the absorption, distribution, metabolism and excretion processes of compound **6** in the body can be observed, as well as whether its regulatory effect on blood glucose level is consistent with the results of cell experiments *in vitro*, so as to more accurately evaluate its hypoglycemic effect. In addition, *in vivo* experiments can also help us to find possible adverse reactions, provide more comprehensive and reliable data support for the subsequent research and development and clinical application of compound **6**, and ensure that its safety and effectiveness are fully verified.

Conclusion

In this study, 13 compounds were isolated and identified from R. radix, including seven monoterpenes **(1-7)** and six phenylethanol **(8-13)**. The structure of the new iridoid **(3)** was characterized by HRMS, 1DNMR, 2D NMR, and IR. Compound **6** effectively improved insulin resistance in HepG2 cells. The mechanism was related to promote the uptake of glucose through the activation of the PI-3K/AKT signaling pathway, and promote the synthesis of glycogen, as well as inhibit gluconeogenesis.

Conflicts of interest

The authors declare that there are no conflicts of interest in this work.

Acknowledgments

This work was funded by National Key R&D Program of China (2022YFF1100300), Major Science and Technology Project of Henan Province (231100310200) and Science and Technology Development Program of Henan Province (222102520035).

Author contributions

Zhenhua Liu: Conceptualization and Writing original draft. **Huihui Zhou**: Project administration and Writing-original draft. **Beibei Yu**: Formal analysis and Project administration. **Shishi Zhang and Xuyang**: Investigation and Validation. **Zhifei Zhang, Changtong Lu, Qiuling Wang, Dongxu Cheng, Yibo Ning and Yanxia Xiong**: Formal analysis and Investigation. **Guangping Lv and Wenyi Kang:** Funding acquisiton and Review & editing.

References

[1] Lee, S., Park, S., & Choi, C. S. Insulin resistance: from mechanisms to therapeutic strategies. *diabetes & metabolism journal*, **2022**, 46: 15–37. https://doi.org/10.4093/dmj.2021.0280

[2] Dong, Z. H., Pan, R. Y., Ren, G. Y., et al. A novel antidiabetic peptide GPAGAP from Andrias davidianus collagen hydrolysates: screening, action mechanism prediction and improving insulin resistance in HepG2 cells. *Food & Medicine Homology*, **2024**, 1: 9420010. https://doi.org/10.26599/FMH.2024.9420010

[3] Wang, T., Wang, Y. Y., Shi, M. Y., et al. Mechanisms of action of natural products on type 2 diabetes. *World Journal of Diabetes*, **2023**, 14: 1603–1620. https://doi.org/10.4239/wjd.v14.i11.1603

[4] Yan, F., Dai, G., & Zheng, X. Mulberry anthocyanin extract ameliorates insulin resistance by regulating PI3K/AKT pathway in HepG2 cells and db/ db mice. *Journal of Nutritional Biochemistry*, **2016**, 36: 68–80. https://doi.org/10.1016/j.jnutbio.2016.07.004

[5] Gandhi, G. R., Jothi, G., Antony, P. J., et al. Gallic acid attenuates high-fat diet fed streptozotocin-induced insulin resistance via partial agonism of PPARγ in experimental type 2 diabetic rats and enhances glucose uptake through translocation and activation of GLUT4 in PI3K/p-AKT signaling pathway. *European Journal of Pharmacology*, **2014**, 745: 201–216. https://doi.org/10.1016/j.ejphar.2014.10.044

[6] Pu, P., Wang, X. A., Salim, M., et al. Baicalein, a natural product, selectively activating AMPKα(2) and ameliorates metabolic disorder in diet-induced mice. *Molecular And Cellular Endocrinology*, **2012**, 362: 128–138. https://doi.org/10.1016/j.mce.2012.06.002

[7] National Pharmacopoeia Committee. Pharmacopoeia of the People's Republic of China. Beijing: China Med Sci Press, **2020**, 129.

[8] Feng, W. S., Li, M., Zheng, X. K., et al. Study on chemical constituents of Immunosuppressive parts from the roots of *Rehmannia glutinosa*. *Chinese Pharmaceutical Journal*, **2014**, 49: 1496–1502.

[9] Li, M. M., Jiang, H. J., & Hao, Y. A. systematic review on botany, processing, application, phytochemistry and pharmacological action of *Radix Rehmnniae*. *Journal of Ethnopharmacology*, **2021**, 285,

114820. https://doi.org/10.1016/j.jep.2021.114820
[10] Chao, C.H., Hsu, J.L., Chen, M.F., et al. Anti-hypertensive effects of *Radix Rehmanniae* and its active ingredients. *Natural Product Research*, **2020**, 34: 1547–1552. https://doi.org/10.1080/14786419.2018.1516660
[11] Sung, Y. Y., Yoon, T., Jang, J. Y., et al. Topical application of *Rehmannia glutinosa* extract inhibits mite allergen-induced atopic dermatitis in NC/Nga mice. *Journal of Ethnopharmacology*, **2011**, 134: 37–44. https://doi.org/10.1016/j.jep.2010.11.050
[12] Zhang, Z., Meng, Y., Guo, Y., et al. *Rehmannia glutinosa* polysaccharide induces maturation of murine bone marrow derived Dendritic cells (BMDCs). *International Journal of Biological Macromolecules*, **2013**, 54: 136–143. https://doi.org/10.1016/j.ijbiomac.2012.12.005
[13] Xu, L., Zhang, W., Zeng, L., et al. *Rehmannia glutinosa* polysaccharide induced an anti-cancer effect by activating natural killer cells. *International Journal of Biological Macromolecules*, **2017**, 105: 680–685. https://doi.org/10.1016/j.ijbiomac.2017.07.090
[14] Lee, B. C., Choi, J. B., Cho, H. J., et al. *Rehmannia glutinosa* ameliorates the progressive renal failure induced by 5/6 nephrectomy. *Journal of Ethnopharmacoloogy*, **2009**, 122: 131–135. https://doi.org/10.1016/j.jep.2008.12.015
[15] Zhu, D., Wang, Y., Du, Q., et al. Cichoric acid reverses insulin resistance and suppresses inflammatory responses in the glucosamine-induced HepG2 cells. *Journal Of Agricultural And Food Chemistry*, **2016**, 63: 10903–10913. https://doi.org/10.1021/acs.jafc.5b04533
[16] Liu, J. J., Lu, J. J., Zhang, J. K., et al. Chemical constituents from the *Rehmanniae Radix Preparata*. *Chinese Pharmaceutical Journal*, **2021**, 56: 449–456.
[17] Tran, T. H. H., Pham, T. M. H., Pham, T. C., et al. Iridoids from the aerial parts of adenosma caeruleum with their nitric oxide inhibitory effects. *Journal of Molecular Structure*, **2024**, 1299: 137–149. https://doi.org/10.1016/j.molstruc.2023.137149
[18] Wang, H., Wu, F. H., Xiong, F., et al. Iridoids from *Neopicrorhiza scrophulariiflora* and their hepatoprotective activities *in vitro*. *Chemical & Pharmaceutical Bulletin*, **2006**, 54: 1144–1149. https://doi.org/10.1248/cpb.54.1144
[19] Wang, H., Ye, W. C., Jiang, R. W., et al. Three new cyclopentanoid monoterpenes from *Picrorhizascrophulariiflora*. *Planta Medica*, **2004**, 70: 382–384. https://doi.org/10.1055/s-2004-818957
[20] Wei, S. F., Meng, L., Xiao, K. Z., et al. Two new ionone glycosides from the roots of *Rehmannia glutinosa Libosch*. *Natural Product Research*, **2015**, 29: 59–63. https://doi.org/10.1080/14786419.2014.958735
[21] Zhang, L., Wen, K., Zhang, Z. Q., et al, et al. 3,4-Dihydroxyphenylethanol ameliorates lipopolysaccharide-induced septic cardiac injury in a murine model. *Open Life Sciences*, **2021**, 16: 1313–1320. https://doi.org/10.1515/biol-2021-0125
[22] Zhang, J. K., Lu, J. J., Li, M., et al. Ionones from the "nine steaming nine sun-drying"*Rehmanniae Radix Praeparata*. *Natural Product Research and Development*, **2021**, 33: 767–772. https://doi.org/10.16333/j.1001-6880.2021.5.007
[23] Li, C. Y., Gao, H., Jiao, W. H., et al. lsolation and identification of quinones constituents from root cortex of *Morinda officinalis*. *Journal of Shenyang Pharmaceutical University*, **2011**, 28: 30–36+60. https://doi.org/10.14066/j.cnki.cn21-1349/r.2011.01.004
[24] Gao, Y., Peng, C. Y., Chen, Y. Y., et al. Studies on the phenylethanoid glycosides from the fresh roots of *Rehmannia glutinosa*. *Journal of Chinese Medicinal Materials*, **2017**, 40: 2073–2076. https://doi.org/10.13863/j.issn1001-4454.2017.09.017
[25] Hong, M. Y., Du, Y. S., Chen, D. D., et al. Martynoside rescues 5-fluorouracil-impaired ribosome biogenesis by stabilizing RPL27A. *Science Bulletin*, **2023**, 68: 15.
[26] Lee, H. D., Kim, J. H., Pang, Q. Q., et al. Antioxidant Activity and acteoside analysis of *Abeliophyllum distichum*. *Antioxidants* (*Basel*). **2020**, 9: 1148. https://doi.org/10.3390/antiox9111148
[27] Anna B., & Jaromir B. A new flavonoid, a new phenylethanoid glycoside and related compounds isolated from the inflorescences of *Plantago lanceolata L*. *Natural Product Research*, **2022**, 36: 3813–3824. https://doi.org/10.1080/14786419.2021.1888289
[28] Tripetch, K., & Ryoji, K. Phenolic glycosides from *Markhamia stipulata*. *Phytochemistry*, **2002**, 59: 557–563. https://doi.org/10.1016/S0031-9422(01)00466-6
[29] Liu, Y. F., Shi, G. R., Wang, X., et al. Nine new compounds from the whole plants of *Rehmannia chingii*. *Journal of Asian Natural Products Research*, **2016**, 18: 509–519. https://doi.org/10.1080/10286020.2016.1173680
[30] Yan, J., Wang, C., Jin, Y., et al. Catalpol ameliorates hepatic insulin resistance in type 2 diabetes through acting on AMPK/NOX4/PI3K/AKT pathway. *Pharmacological Research*, **2018**, 130: 466–480. https://doi.org/10.1016/j.phrs.2017.12.026
[31] Xu, D. Q., Huang, X. F., Hassan, H. M., et al. Hypoglycaemic effect of catalpol in a mouse model of high-fat diet-induced prediabetes. *Applied Physiology Nutrition and Metabolism*, **2020**, 45: 1127–1137. https://doi.org/10.1139/apnm-2020-0075
[32] Xu, D. Q., Wang, L., Jiang, Z., et al. A new hypoglycemic mechanism of catalpol revealed by enhancing MyoD/MyoG-mediated myogenesis. *Life Sciences*, **2018**, 209: 313–323. https://doi.org/10.1016/j.lfs.2018.08.028
[33] Yap, K. H., Yee, G. S., Candasamy, M., et al. Catalpol ameliorates insulin sensitivity andmitochondrial respiration in skeletal muscle of type-2 diabetic mice through insulin signaling pathway and AMPK/SIRT1/PGC-1*α*/PPAR-*γ* activation. *Biomolecules*, **2020**, 10: 1360. https://doi.org/10.3390/biom10101360
[34] Liu, Z. H., Xu, L. T., Xu, X. Q., et al. Effects and mechanisms of iridoid glycosides from *Patrinia scabiosaefolia* on improving insulin resistance in 3T3-L1 adipocytes. *Food And Chemical Toxicology*, **2019**, 134: 110806. https://doi.org/10.1016/j.fct.2019.110806
[35] Liu, Z. H., Wang, M. K., Liu, Y. H., et al. Patrinoside and Patrinoside A from *Patrinia scabiosaefolia* improve insulin resistance by inhibiting NF-*κ*B, MAPK pathways and oxidative stress in RAW264.7 and 3T3-L1 cells. *Oxidative Medicine and Cellular Longevity*, **2023**, 9069645. https://doi.org/10.1155/2023/9069645
[36] Liu, Z. H., Meng, L. J., Wang, M. K., et al. New iridoids from *Patrinia scabiosaefolia* and their hypoglycemic effects by activating PI3K/AKT signaling pathway. *Fitoterapia*, **2023**, 165: 105423. https://doi.org/10.1016/j.fitote.2022.105423
[37] Cao, R., Tian, H., Zhang, Y., et al. Signaling pathways and intervention for therapy of type 2 diabetes mellitus. *MedComm*, **2020**, 4: e283. https://doi.org/10.1002/mco2.283
[38] Thu, V. K., Thoa, N. T., Hien, N. T. T., et al. Iridoid glycosides link with phenylpropanoids from *Rehmannia glutinosa*. *Natural Product Research*, **2022**, 36: 5370–5375. https://doi.org/10.1080/14786419.2021.1931189
[39] Uddin, M. J., Russo, D., Haque, M. A., et al. Bioactive abietane-type diterpenoid glycosides from leaves of *Clerodendrum infortunatum* (*Lamiaceae*). *Molecules*, **2021**, 26: 4121. https://doi.org/10.3390/molecules26144121
[40] Ivanka, K. K., Liliya, V. M., Monika, N. T., et al. Leucosceptoside A from devil's claw modulates psoriasis-like inflammation via suppression of the PI3K/AKT signaling pathway in keratinocyte. *Molecules*, **2021**, 26: 7014. https://doi.org/10.3390/molecules26227014
[41] Hong, M., Chen, D., Hong, Z., et al. *Ex vivo* and *in vivo* chemoprotective activity and potential mechanism of martynoside against 5-fluorouracil-induced bone marrow cytotoxicity. *Biomed Pharmacother*, **2021**, 138: 111501. https://doi.org/10.1016/j.biopha.2021.111501